

Articles

Synthesis and Studies on the Reactivities of Dicyclopentadienylytterbium Derivatives Containing Carbazolate and Pyrazolate Ligands

Jie Zhang,[†] Ruifang Cai,[†] Linhong Weng,[†] and Xigeng Zhou^{*,†,‡}

Molecular Catalysis and Innovative Material Laboratory, Department of Chemistry, Fudan University, Shanghai 200433, People's Republic of China, and State Key Laboratory of Organometallic Chemistry, Shanghai 200032, People's Republic of China

Received July 11, 2003

Two ytterbocene derivatives containing aromatic nitrogen ligands, $(C_5H_5)_2YbCbz(THF)$ (**1**) and $(C_5H_5)_2YbPzMe_2(THF)$ (**4**), were synthesized, and their reactivities toward *N,N*-diisopropylcarbodiimide, phenyl isothiocyanate, and phenyl isocyanate were studied. Abstraction of cyclopentadienyl from $(C_5H_5)_3Yb$ with 1 equiv of carbazole (HCbz) in THF at room temperature gives **1**. Reaction of **1** with *N,N*-diisopropylcarbodiimide ($^iPrN=C=N^iPr$) results in monoinsertion of $^iPrN=C=N^iPr$ into the Yb–N(Carbazolate) bond, yielding the ytterbocene guanidinate $(C_5H_5)_2Yb[{}^iPrN=C(Cbz)\cdots N^iPr]$ (**2**), while treatment of **1** with 1 equiv of phenyl isothiocyanate (PhNCS) gives the unexpected monocyclopentadienylytterbium complex $(C_5H_5)Yb[S\cdots C(Cbz)\cdots NPh]_2(THF)$ (**3**) and $(C_5H_5)_3Yb(THF)$, which may be rationalized by the ligand rearrangement of the monoinsertion product $(C_5H_5)_2Yb[S\cdots C(Cbz)\cdots NPh]$. $(C_5H_5)_3Yb$ reacts with 3,5-dimethylpyrazole (HPzMe₂) in a 1:1 ratio at ambient temperature to form complex **4**. Reaction of **4** with PhNCO gives the insertion product $(C_5H_5)_2Yb[OC(=NPh)-PzMe_2](THF)$ (**5**). In contrast to **1**, however, complex **4** does not react with $^iPrNCN^iPr$ under the same conditions. All these complexes were characterized by elemental analysis and spectroscopic properties. The structures of complexes **2**–**5** were also determined by X-ray single-crystal diffraction analyses. These reactions present the first example of 1,3-heterocumulene insertions into the Ln–N(aromatic ring) bond and provide a new strategy for introducing a substituent at the nitrogen atom of organic heterocycle compounds.

Introduction

The carbazolate anion is an interesting ligand, because it can attach to a metal by several different modes, such as η^1 , η^3 , and η^5 coordination modes.¹ Although their organometallic complexes have been extensively investigated in main-group-metal and transition-metal chemistry,² knowledge about their lanthanide complexes is rather limited; only a few divalent lanthanide complexes with carbazolate ligands have been synthesized to date.³

On the other hand, there is currently considerable interest in studying the reactivities of the Ln–N bond of organolanthanide complexes, due to their applications in organic synthesis and catalysis.⁴ However, research efforts have been primarily focused on organolanthanide amido complexes (amido = NR^1R^2 ; $R^1, R^2 = H$, alkyl, aryl, silyl), and the reactivity of organolanthanide complexes containing aromatic nitrogen ligands has been much less studied.^{5,6e} In most cases, aromatic nitrogen ligands are only typically ancillary ligands

[†] Fudan University.

[‡] State Key Laboratory of Organometallic Chemistry.

(1) (a) Hacker, R.; Kaufmann, E.; Schleyer, P. v. R.; Mahdi, W.; Dietrich, H. *Chem. Ber.* **1987**, *120*, 1533. (b) Gregory, K.; Bremer, M.; Schleyer, P. v. R.; Klusener, P. A. A.; Brandsma, L. *Angew. Chem., Int. Ed. Engl.* **1989**, *28*, 1224. (c) Mosges, G.; Hampel, F.; Kaupp, M.; Schleyer, P. v. R. *J. Am. Chem. Soc.* **1992**, *114*, 10880.

(2) (a) Riley, P. N.; Fanwick, P. E.; Rothwell, I. P. *Dalton* **2001**, 181. (b) Riley, P. N.; Parker, J. R.; Fanwick, P. E.; Rothwell, I. P. *Organometallics* **1999**, *18*, 3679. (c) Riley, P. N.; Profflet, R. D.; Salberg, M. M.; Fanwick, P. E.; Rothwell, I. P. *Polyhedron* **1998**, *17*, 773. (d) Beswick, M. A.; Harmer, C. N.; Raithby, P. R.; Steiner, A.; Verhorevoort, K. L.; Wright, D. S. *J. Chem. Soc., Dalton Trans.* **1997**, 2029. (e) Bock, H.; Arad, C.; Nather, C.; Havlas, Z. *J. Organomet. Chem.* **1997**, *548*, 115. (f) Riley, P. N.; Profflet, R. D.; Fanwick, P. E.; Rothwell, I. P. *Organometallics* **1996**, *15*, 5502. (g) Lambert, C.; Hampel, F.; Schleyer, P. v. R. *Angew. Chem., Int. Ed. Engl.* **1992**, *31*, 1209.

(3) (a) Evans, W. J.; Rabe, G. W.; Ziller, J. W. *Organometallics* **1994**, *13*, 1641. (b) Deacon, G. B.; Forsyth, C. M.; Gatehouse, B. M.; White, P. A. *Aust. J. Chem.* **1990**, *43*, 795. (c) Deacon, G. B.; Forsyth, C. M.; Newham, R. H.; *Polyhedron* **1987**, *6*, 1143.

(4) (a) Molander, G. A.; Romero, J. A. C. *Chem. Rev.* **2002**, *102*, 2161. (b) Schumann, H.; Meese-Marktscheffel, J. A.; Esser, L. *Chem. Rev.* **1995**, *95*, 865. (c) Arredondo, V. M.; Tian, S.; McDonald, F. E.; Marks, T. J. *J. Am. Chem. Soc.* **1999**, *121*, 3633. (d) Tian, S.; Arredondo, V. M.; Marks, T. J. *Organometallics* **1999**, *18*, 2125. (e) Obora, Y.; Ohta, T.; Stern, C. L.; Marks, T. J. *J. Am. Chem. Soc.* **1997**, *119*, 3745.

(5) (a) Fedushkin, I. L.; Petrovskaya, T. V.; Girgsdies, F.; Kohn, R. D.; Bochkarev, M. N.; Schumann, H. *Angew. Chem., Int. Ed.* **1999**, *38*, 2262. (b) Evans, W. J.; Drummond, D. K. *J. Am. Chem. Soc.* **1994**, *116*, 2600. (c) Schumann, H.; Loebel, J.; Pickardt, J.; Qian, C.; Xie, Z. *Organometallics* **1991**, *10*, 215. (d) Schumann, H.; Lee, P. R.; Dietrich, A. *Chem. Ber.* **1990**, *123*, 131. (e) Evans, W. J.; Gonzales, S. L.; Ziller, J. W. *J. Am. Chem. Soc.* **1989**, *111*, 3329.

which stabilize and construct but do not participate in organometallic reactions.^{1–3,5}

We have recently been interested in the reactivities of organolanthanide complexes toward unsaturated organic small molecules.⁶ The investigation results in this field indicate that the occurrence of the insertion strongly depends on the degree of the steric saturation around the center metal ion and the nature of the ligands. In a continuation of our recent investigation of the lanthanide-ligand insertion and in order to learn more about the aromatic nitrogen heterocycle anion as a ligand, we herein report the synthesis of trivalent ytterbocene carbazolate and pyrazolate complexes as well as their reactivities toward carbodiimide, isocyanate, and isothiocyanate, which present the first example of 1,3-heterocumulene insertions into the Ln–N(aromatic ring) bond and provide a new strategy for introducing a substituent at the nitrogen atom of organic heterocycles via formation of a new C–N(ring) bond.

Experimental Section

General Procedure. All operations involving air- and moisture-sensitive compounds were carried out under an inert atmosphere of purified argon or nitrogen using standard Schlenk techniques. The solvents of THF, toluene, and *n*-hexane were refluxed and distilled over sodium benzophenone ketyl under nitrogen immediately prior to use. (C₅H₅)₃Yb was prepared by the literature procedure.⁷ Carbazole, 3,5-dimethylpyrazole, *N,N*-diisopropylcarbodiimide, and phenyl isocyanate were purchased from Aldrich and were used without purification. Elemental analyses for C, H, and N were carried out on a Rapid CHN-O analyzer. Infrared spectra were obtained on a Nicolet FT-IR 360 spectrometer with samples prepared as Nujol mulls. Mass spectra were recorded on a Philips HP5989A instrument operating in EI mode. Crystalline samples of the respective complexes were rapidly introduced by the direct inlet techniques with a source temperature of 200 °C. The *m/z* values are referred to the isotopes ¹²C, ¹H, ¹⁴N, ¹⁶O, and ¹⁷⁴Yb. ¹H NMR data were obtained on a Bruker DMX-500 NMR spectrometer and were referenced to residual aryl protons in C₆H₆ (δ 7.16).

Synthesis of (C₅H₅)₂YbCbz(THF) (1). (C₅H₅)₃Yb (2.35 g, 6.38 mmol) and carbazole (1.07 g, 6.39 mmol) were mixed in 100 mL of THF. The solution slowly turned from dark green to dark red over several hours. After the mixture was stirred for 24 h at room temperature, all volatile substances were removed under vacuum to give a red powder. Yield: 3.32 g (90%). Recrystallization of the powder from the mixture of THF and toluene gave **1** as red crystals. Anal. Calcd for C₂₆H₂₆NOYb: C, 57.67; H, 4.84; N, 2.59. Found: C, 57.34; H, 4.69; N, 2.64. ¹H NMR: δ 6.29–7.99 (m, 8H), 2.11 (s, 10H). IR (Nujol, cm⁻¹): 3175 w, 1620 s, 1584 m, 1336 m, 1322 m, 1263 s, 1122 m, 1148 s, 1074 s, 1015 s, 959 m, 903 m, 848 s, 759 m, 663 w. EI-MS (*m/z* (fragment, relative intensity (%))): 470 (M – THF, 8), 304 (Cp₂Yb, 46), 167 (CbzH, 100), 72 (THF, 17), 65 (CpH, 66).

Synthesis of (C₅H₅)₂Yb[ⁱPrN–C(Cbz)–NⁱPr] (2). To a 30 mL THF solution of **1** (0.946 g, 1.76 mmol) was slowly added *N,N*-diisopropylcarbodiimide (0.222 g, 1.76 mmol) dropwise

at room temperature, and the mixture was stirred for several hours. The dark red solution became yellow-orange. After it was stirred overnight, the reaction solution was concentrated by reduced pressure to about 2 mL. Addition of 20 mL of *n*-hexane resulted in the precipitation of a yellow solid. The resulting mixture was centrifuged, and the solution was decanted. The precipitate was washed with *n*-hexane and dried under vacuum to afford a yellow powder. Recrystallization of the powder from the solvent mixture of THF and *n*-hexane gave **2** as yellow crystals. Yield: 0.60 g (57%). Anal. Calcd for C₂₉H₃₂N₃Yb: C, 58.48; H, 5.42; N, 7.05. Found: C, 58.23; H, 5.40; N, 7.11. ¹H NMR: δ 6.29–7.98 (m, 8H), 3.57 (s, 5H), 2.49–2.69 (m, 2H), 0.89–1.42 (m, 12H), 0.4 (s, 5H). IR (Nujol, cm⁻¹): 3175 w, 1666 s, 1620 s, 1597s, 1514 m, 1402 m, 1331 m, 1312 m, 1233 s, 1198 m, 1170 s, 1148 m, 1058 s, 1011 s, 971 s, 770 s, 748 s, 684 m, 617 w. EI-MS (*m/z* (fragment, relative intensity (%))): 596 (M, 13), 581 (M – CH₃, 24), 430 (M – Cbz, 49), 304 (Cp₂Yb, 47), 166 (Cbz, 37), 43 (Bu, 51).

Synthesis of (C₅H₅)₂Yb[S–C(Cbz)–NPh]₂(THF) (3). To a 20 mL THF solution of **1** (0.408 g, 0.76 mmol) was slowly added phenyl isocyanate (0.104 g, 0.77 mmol) dropwise at –30 °C. After it was stirred for 30 min at low temperature, the mixture was slowly warmed to room temperature and stirred for several hours. Removal of the solvent left a yellow oily solid. The resulting oily solid was extracted with 30 mL of toluene. The extract was evaporated to ca. 5 mL, and yellow crystals of **3** were slowly formed at room temperature. Yield: 0.25 g (36% based on Yb). Anal. Calcd for C₄₇H₃₉N₄O₂Yb: C, 61.83; H, 4.31; N, 6.14. Found: C, 61.91; H, 4.30; N, 6.23. ¹H NMR: δ 6.30–8.02 (m, 10H), 3.57 (s, 5H), 0.93–2.69 (b, 24H). IR (Nujol, cm⁻¹): 3175 w, 1664 m, 1616 w, 1595 s, 1574 m, 1518 s, 1320 m, 1301 m, 1225 s, 1203 m, 1154 s, 1091 s, 1071 m, 1009 s, 895 m, 851 m, 770 s, 747 s, 690 s, 663 w. EI-MS (*m/z* (fragment, relative intensity (%))): 304 (Cp₂Yb, 15), 286 (L + H, 28), 167 (Cbz, 52), 119 (L – Cbz, 23), 71 (THF – H, 100), 66 (CpH, 61) (L = SC(Cbz)NPh). Further crystallization by diffusion of *n*-hexane into the above mother liquor yielded a mixture of yellow crystals and dark crystals. The latter was identified to be (C₅H₅)₃Yb(THF) by comparison of the X-ray crystallographic analysis data with literature values.^{5c}

Synthesis of (C₅H₅)₂YbPzMe₂(THF) (4). (C₅H₅)₃Yb (0.968 g, 2.63 mmol) and 3,5-dimethylpyrazole (0.252 g, 2.63 mmol) were mixed in 50 mL of THF. The solution slowly turned from dark green to yellow over several hours. After the mixture was stirred overnight at room temperature, all volatile substances were removed under vacuum to give a yellow powder. Recrystallization of the powder from the mixture of THF and toluene gave **4** as orange crystals. Yield: 0.88 g (72%). Anal. Calcd for C₁₉H₂₅N₂OYb: C, 48.51; H, 5.36; N, 5.95. Found: C, 48.39; H, 5.31; N, 6.02. IR (Nujol, cm⁻¹): 3175 w, 3090 w, 1655 s, 1602 m, 1570 s, 1571 s, 1347 m, 1250 m, 1171 s, 1109 s, 1073 s, 1013 s, 963 m, 922 s, 872 s, 772 s, 675 m, 661 w. EI-MS (*m/z* (fragment, relative intensity (%))): 399 (M – THF, 15), 334 (M – THF – Cp, 28), 267 (M – THF – 2Cp, 38), 96 (HPzMe₂, 33), 65 (Cp, 100).

Synthesis of (C₅H₅)₂Yb[OC(=NPh)PzMe₂](THF) (5). To a 30 mL THF solution of **4** (0.534 g, 1.13 mmol) was slowly added phenyl isocyanate (0.135 g, 1.14 mmol) dropwise at room temperature, and the mixture was stirred overnight. The reaction solution was concentrated to ca. 3 mL by reduced pressure. Yellow crystals of **5** were obtained at –20 °C for several days. Yield: 0.43 g (64%). Anal. Calcd for C₂₆H₃₀N₃O₂Yb: C, 52.97; H, 5.13; N, 7.13. Found: C, 52.88; H, 5.21; N, 7.04. ¹H NMR: δ 9.27 (s, 1H), 7.01–7.73 (m, 5H), 5.17 (b, 5H), 2.49–2.69 (m, 4H), 2.04 (b, 5H), 1.36 (s, 6H), 0.92–1.20 (m, 4H). IR (Nujol, cm⁻¹): 3175 w, 1655 s, 1590 s, 1529 s, 1301 m, 1268 s, 1179 m, 1155 s, 1126 m, 1067 s, 1020 s, 984 m, 917 s, 873 m, 770 m, 698 s, 670 w, 630 w, 585 w. EI-MS (*m/z* (fragment, relative intensity (%))): 590 (M, 5), 518 (M – THF, 2), 399 (M – THF – PhNCO, 11), 334 (M – THF – PhNCO –

(6) (a) Zhang, J.; Cai, R. F.; Weng, L. H.; Zhou, X. G. *J. Organomet. Chem.* **2003**, *672*, 94. (b) Zhang, J.; Ruan, R. Y.; Saho, Z. H.; Cai, R. F.; Weng, L. H.; Zhou, X. G. *Organometallics* **2002**, *21*, 1420. (c) Zhou, X. G.; Zhu, M. *J. Organomet. Chem.* **2002**, *647*, 28. (d) Zhou, X. G.; Zhang, L. B.; Zhu, M.; Cai, R. F.; Weng, L. H.; Huang, Z. X.; Wu, Q. *J. Organometallics* **2001**, *20*, 5700. (e) Zhou, X. G.; Huang, Z. E.; Cai, R. F.; Zhang, L. B.; Zhang, L. X.; Huang, X. Y. *Organometallics* **1999**, *18*, 4128.

(7) Wilkinson, G.; Birmingham, J. M. *J. Am. Chem. Soc.* **1954**, *78*, 42.

Table 1. Crystal and Data Collection Parameters of Complexes 2–5

	2	3	4	5
formula	C ₂₉ H ₂₂ N ₃ Yb	C ₄₇ H ₃₉ N ₄ OS ₂ Yb	C ₁₉ H ₂₅ N ₂ OYb	C ₂₆ H ₃₀ N ₃ O ₂ Yb
mol wt	595.62	912.98	470.45	589.57
cryst color	yellow	yellow	orange	yellow
cryst dimens (mm)	0.45 × 0.40 × 0.10	0.20 × 0.15 × 0.10	0.20 × 0.15 × 0.10	0.40 × 0.20 × 0.20
cryst syst	monoclinic	triclinic	monoclinic	monoclinic
space group	<i>P</i> 2 ₁ / <i>n</i>	<i>P</i> 1	<i>P</i> 2 ₁ / <i>c</i>	<i>P</i> 2 ₁ / <i>c</i>
unit cell dimens				
<i>a</i> (Å)	9.535(3)	12.957(11)	8.1826(15)	17.804(2)
<i>b</i> (Å)	8.276(2)	14.860(12)	14.503(3)	7.9199(9)
<i>c</i> (Å)	32.545(9)	14.880(12)	16.187(3)	18.910(2)
α (deg)		74.266(12)		
β (deg)	96.933(4)	71.540(11)	100.886(3)	114.7940(10)
γ (deg)		66.508(11)		
<i>V</i> (Å ³)	2549.6(12)	1886.3(6)	1886.3(6)	2420.7(5)
<i>Z</i>	4	2	4	4
<i>D_c</i> (g cm ⁻³)	1.552	1.234	1.657	1.618
μ (mm ⁻¹)	3.689	2.021	4.963	3.890
<i>F</i> (000)	1188	918	924	1172
radiation		Mo K α (λ = 0.710 730 Å)		
temp (K)	298.2	298.2	298.2	298.2
scan type	ω -2 θ	ω -2 θ	ω -2 θ	ω -2 θ
θ range (deg)	2.17–25.01	1.46–25.01	2.53–25.01	2.17–26.76
<i>h, k, l</i> range	-10 ≤ <i>h</i> ≤ 11 -9 ≤ <i>k</i> ≤ 9 -33 ≤ <i>l</i> ≤ 38	-15 ≤ <i>h</i> ≤ 15 -17 ≤ <i>k</i> ≤ 17 -16 ≤ <i>l</i> ≤ 17	-9 ≤ <i>h</i> ≤ 9 -17 ≤ <i>k</i> ≤ 17 -15 ≤ <i>l</i> ≤ 19	-17 ≤ <i>h</i> ≤ 22 -9 ≤ <i>k</i> ≤ 9 -23 ≤ <i>l</i> ≤ 23
no. of rflns measd	10 294	11 683	7801	11 433
no. of unique rflns	4479 (<i>R</i> _{int} = 0.0704)	11 683 (<i>R</i> _{int} = 0.0000)	3308 (<i>R</i> _{int} = 0.0350)	5092 (<i>R</i> _{int} = 0.0265)
completeness to θ (%)	99.8 (θ = 25.01)	96.4 (θ = 25.01)	99.5 (θ = 25.01)	99.2 (θ = 26.76)
max and min rtransmissn	0.7093 and 0.2876	0.8234 and 0.6879	0.6367 and 0.4368	0.5101 and 0.3052
refinement method		full-matrix least squares on <i>F</i> ²		
no. of data/restraints/params	4479/0/302	11 683/60/396	3308/30/243	5092/0/291
goodness of fit on <i>F</i> ²	0.933	0.978	1.035	0.944
final <i>R</i> indices (<i>I</i> > 2 σ (<i>I</i>))	<i>R</i> 1 = 0.0504 w <i>R</i> 2 = 0.1135	<i>R</i> 1 = 0.0885 w <i>R</i> 2 = 0.2152	<i>R</i> 1 = 0.0394 w <i>R</i> 2 = 0.0869	<i>R</i> 1 = 0.0228 w <i>R</i> 2 = 0.0505
<i>R</i> indices (all data)	<i>R</i> 1 = 0.0712 w <i>R</i> 2 = 0.1202	<i>R</i> 1 = 0.1157 w <i>R</i> 2 = 0.2338	<i>R</i> 1 = 0.0505 w <i>R</i> 2 = 0.0918	<i>R</i> 1 = 0.0292 w <i>R</i> 2 = 0.0519
largest diff peak and hole (e Å ⁻³)	2.015 and -1.219	2.215 and -1.422	1.083 and -1.034	0.855 and -0.455

Cp, 28), 269 (YbPzMe₂, 21), 119 (PhNCO, 85), 96 (HPzMe₂, 72), 72 (THF, 11), 66 (CpH, 100).

X-ray Data Collection, Structure Determination, and Refinement. Suitable single crystals of complexes 2–5 were sealed under argon in Lindemann glass capillaries for X-ray structural analysis. Diffraction data were collected on a Bruker SMART Apex CCD diffractometer using graphite-monochromated Mo K α (λ = 0.710 73 Å) radiation. During the intensity data collection, no significant decay was observed. The intensities were corrected for Lorentz–polarization effects and empirical absorption with the SADABS program.⁸ The structures were solved by direct methods using the SHELXL-97 program.⁹ All non-hydrogen atoms were found from the difference Fourier syntheses. The H atoms were included in calculated positions with isotropic thermal parameters related to those of the supporting carbon atoms but were not included in the refinement. All calculations were performed using the Bruker Smart program. A summary of the crystallographic data and selected experimental information is given in Table 1.

(a) (C₅H₅)₂Yb[PrN–C(Cbz)–N'Pr] (2). Frames were integrated to the maximum 2 θ angle of 50.02° with the Siemens SAINT program to yield a total of 10 294 reflections, of which 4479 were independent (*R*_{int} = 0.0704). Laue symmetry revealed a monoclinic crystal system, and the final unit cell parameters were determined from the full-matrix least-squares refinement on *F*² of three-dimensional centroids of 4479 reflections. Further refinement led to final convergence at *R* = 0.0504.

(b) (C₅H₅)₂Yb[S–C(Cbz)–NPh]₂(THF) (3). Frames were integrated to the maximum 2 θ angle of 50.02° with the

Siemens SAINT program to yield a total of 11 683 reflections. All of them were independent. Laue symmetry revealed a triclinic crystal system, and the final unit cell parameters were determined from the full-matrix least-squares refinement on *F*² of three-dimensional centroids of 11 683 reflections. Further refinement led to final convergence at *R* = 0.0885.

(c) (C₅H₅)₂YbPzMe₂(THF) (4). Frames were integrated to the maximum 2 θ angle of 50.02° with the Siemens SAINT program to yield a total of 7801 reflections, of which 3308 were independent (*R*_{int} = 0.0350). Laue symmetry revealed a monoclinic crystal system, and the final unit cell parameters were determined from the full-matrix least-squares refinement on *F*² of three-dimensional centroids of 3308 reflections. Further refinement led to final convergence at *R* = 0.0394.

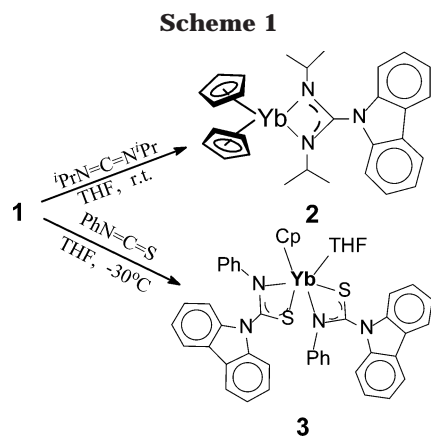
(d) (C₅H₅)₂Yb[OC(=NPh)PzMe₂](THF) (5). Frames were integrated to the maximum 2 θ angle of 53.52° with the Siemens SAINT program to yield a total of 11 433 reflections, of which 5092 were independent (*R*_{int} = 0.0265). Laue symmetry revealed a monoclinic crystal system, and the final unit cell parameters were determined from the full-matrix least-squares refinement on *F*² of three-dimensional centroids of 5092 reflections. Further refinement led to final convergence at *R* = 0.0228.

Results and Discussion

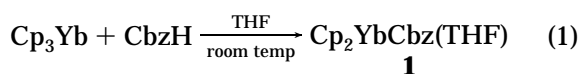
Synthesis and Characterization of the Trivalent Ytterbocene Carbazolate Complex (C₅H₅)₂YbCbz(THF) (1). The known divalent lanthanide carbazolate complex was synthesized by the metathetic reaction of SmI₂(THF)₄ with KCbz^{5a} or the protolysis reactions of Ln(C₆F₆)₂ (Ln = Yb, Eu) with carbazole (CbzH).^{5b,c} To our knowledge, no trivalent organolanthanide carbazolate was reported. Here we synthesized complex 1 by

(8) Sheldrick, G. M. SADABS, Program for Empirical Absorption Correction; University of Göttingen, Göttingen, Germany, 1998.

(9) Sheldrick, G. M. SHELXL-97, Program for the Refinement of Crystal Structures; University of Göttingen, Göttingen, Germany, 1997.



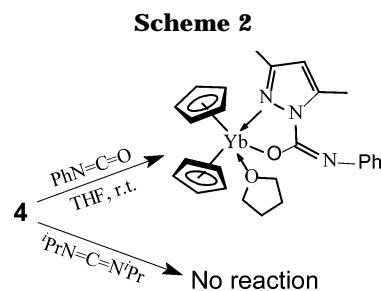
the protolysis reaction of $(C_5H_5)_3Yb$ with 1 equiv of CbzH in THF at room temperature, as shown in the reaction equation



Complex **1** is air- and moisture-sensitive. It is soluble in THF and toluene and slightly soluble in *n*-hexane. Complex **1** has been characterized by elemental analysis and infrared, 1H NMR, and mass spectroscopy, which were in good agreement with the proposed formula. The mass spectrum of **1** displays a series of peaks clearly representing fragments derived from the parent molecule. In the IR spectra, complex **1** exhibits two characterized absorptions at 1620 and 1584 cm^{-1} , which may be attributed to the ring stretching modes of the carbazolate ligand^{5a} and two well-defined bands at 1074 and 903 cm^{-1} for the coordinated THF. Unfortunately, the crystal structure of **1** has not been solved by X-ray analysis due to poor crystal quality.

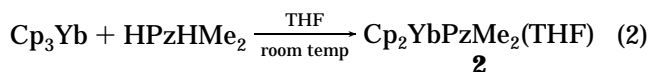
Reactions of Complex 1 with $iPrN=C=NiPr$ and PhNCS. Recently, we and other groups have found that carbodiimide readily inserts into the $Ln-NR_2$ ($R = \text{alkyl, silyl}$) σ -bonds of lanthanide amido complexes, yielding the corresponding guanidinate complexes.^{6a,10} However, it has been unclear up to now whether carbodiimide molecules can be inserted into the $Ln-N(\text{aromatic ring})$ bond. To study the effect of the nature of the organic nitrogen ligand on the insertion and explore the reactivity of complex **1**, we first investigated the reaction of **1** with carbodiimide. When *N,N*-diisopropylcarbodiimide was added to a THF solution of **1** at room temperature, the corresponding guanidinate complex $(C_5H_5)_2Yb[iPrN=C(NiPr)_2](THF)$ (**2**) was obtained in moderate yield, indicating that one carbodiimide molecule is inserted into the $Ln-N(Cbz)$ bond (Scheme 1).

To gain more insight into the reactivity of complex **1**, the reaction of **1** with phenyl isothiocyanate was also studied. Significantly, it is found that reaction of complex **1** with 1 equiv of phenyl isothiocyanate results in the formation of the unexpected product $(C_5H_5)Yb[S=C(NPh)_2](THF)$ (**3**) along with the formation of a small amount of $(C_5H_5)_3Yb(THF)$. Presumably, complex **3** might result from the rearrangement of the monoinsertion product $(C_5H_5)_2Yb[S=C(NPh)](THF)$.



However, attempts to isolate the intermediate $(C_5H_5)_2Yb[S=C(Cbz)NPh]$ were unsuccessful at room temperature. In organolanthanide chemistry, mono(cyclopentadienyl)lanthanide derivatives are usually thermodynamically unstable, liable to rearrange to the more thermodynamic stable bis(cyclopentadienyl)lanthanide derivatives due to the large radius of the metal ion and high coordination number.¹¹ However, very few ligand rearrangement reactions from bis(cyclopentadienyl)lanthanide derivatives to mono(cyclopentadienyl)lanthanide derivatives have been observed.^{5c}

Synthesis of the Ytterbocene Pyrazolate Complex $(C_5H_5)_2YbPzMe_2(THF)$ (4**).** To further study the reactivity of organolanthanides containing aromatic nitrogen ligands, we have also synthesized the complex $(C_5H_5)_2YbPzMe_2(THF)$ (**4**) by the reaction of $(C_5H_5)_3Ln$ with HPzMe₂ in THF at room temperature (eq 2).



Reaction of Complex 4 with PhNCO. Although organometallic pyrazolates have been extensively investigated, examples of $M-N$ insertion based on the chelating pyrazolate ligand are very rare.^{12,16b} To further investigate the effects of the steric factors and bonding mode of the aromatic nitrogen ligand on the insertion, reactions of complex **4** with isocyanate and carbodiimide, respectively, have been studied. The results indicate that PhNCO can be monoinserted into the $Ln-N(\eta^2\text{-pyrazolate})$ bond of **4** to yield $(C_5H_5)_2Yb[OC(=NPh)PzMe_2](THF)$ (**5**) (Scheme 2), but no further reaction involving phenyl isocyanate was observed, even in the presence of excess PhNCO with a higher reaction temperature and a longer reaction time. This is different from the observation of PhNCO insertion into the $Ln-N$ σ -bond of $(CH_3C_5H_4)_2Ln(NiPr_2)(THF)$ ($Ln = Y, Yb, Er$), where excess PhNCO can be catalyzed to give a polymer.¹³ This may be attributed to the differences of steric hindrance and the bonding mode between **5** and $(CH_3C_5H_4)_2Ln[OC(NiPr_2)NPh](THF)$, as shown in Figure 4 (vide infra).

Notably, in contrast to organolanthanide amido complexes,^{6a,10} complex **4** does not react with *N,N*-diisopropylcarbodiimide under the same conditions. This may be attributed to the chelating coordination mode of the pyrazolate ligand, which is disfavored for the interaction of the carbodiimide molecule with the central metal and results in a decrease in the $Ln-N$ bond reactivity.^{6e}

(11) Arndt, S.; Okuda, J. *Chem. Rev.* **2002**, *102*, 1953.

(12) Ahn, S.; Mayr, A. *J. Am. Chem. Soc.* **1996**, *118*, 7408.

(13) Mao, L.; Shen, Q.; Xue, M.; Sun, J. *Organometallics* **1997**, *15*, 33711.

(10) Giesbrecht, G. R.; Whitener, G. D.; Arnold, J. *Dalton* **2001**, 923.

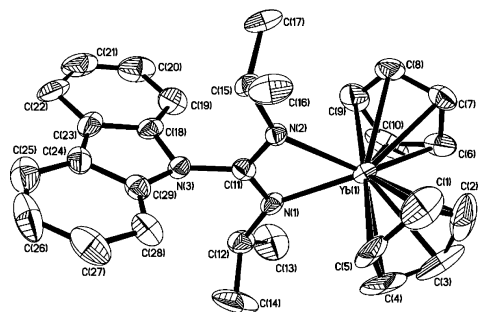


Figure 1. ORTEP diagram of **2** with the probability ellipsoids drawn at the 30% level. Hydrogen atoms are omitted for clarity.

Table 2. Selected Bond Lengths (Å) and Angles (deg) for 2

Yb(1)–N(1)	2.292(6)	Yb(1)–C(10)	2.566(9)
Yb(1)–N(2)	2.305(6)	Yb(1)–C(8)	2.580(9)
Yb(1)–C(5)	2.535(10)	Yb(1)–C(7)	2.590(9)
Yb(1)–C(9)	2.545(10)	N(1)–C(11)	1.297(10)
Yb(1)–C(4)	2.545(12)	N(2)–C(11)	1.303(9)
Yb(1)–C(3)	2.546(12)	N(3)–C(29)	1.367(10)
Yb(1)–C(6)	2.553(10)	N(3)–C(18)	1.396(11)
Yb(1)–C(2)	2.561(11)	N(3)–C(11)	1.431(9)
Yb(1)–C(1)	2.562(11)		
N(1)–Yb(1)–N(2)	58.0(2)	N(1)–C(11)–N(2)	118.1(7)
C(11)–N(1)–Yb(1)	92.3(5)	N(1)–C(11)–N(3)	120.5(7)
C(11)–N(2)–Yb(1)	91.6(5)	N(2)–C(11)–N(3)	121.4(7)
C(29)–N(3)–C(18)	108.8(7)	N(1)–C(11)–Yb(1)	58.8(4)
C(29)–N(3)–C(11)	125.7(6)	N(2)–C(11)–Yb(1)	59.3(4)
C(18)–N(3)–C(11)	122.0(7)	N(3)–C(11)–Yb(1)	178.6(5)

Complexes **2–5** were characterized by elemental analysis and spectroscopic properties, which were in good agreement with the proposed structures. Their mass spectra display the molecular ion peaks or a series of peaks clearly representing fragments derived from the parent molecule. Significantly, the MS data of **5** show that the loss of the PhNCO fragment occurs more readily than the direct loss of the PzMe₂ group. This differs from the observed results in other PhNCO insertion products.^{6d,13} In the IR spectra of **2**, the characterized absorption at ca. 2100 cm⁻¹ for the ν_{as}(N=C=N) stretch of free carbodiimide is absent, but a new strong band at ca. 1666 cm⁻¹ attributable to the delocalized –N=C=N– stretching mode is present.¹⁴ The structures of complexes **2–5** were further confirmed by X-ray single-crystal structure determinations.

Crystal Structures of 2–5. The X-ray structural analysis results show that **2** (Figure 1, Table 2) is a solvent-free monomer with the ytterbium atom bonded to two η⁵-cyclopentadienyl rings and one chelating guanidinate ligand to form a distorted-tetrahedral geometry. The coordination number of the central Yb³⁺ is 8. As expected, the coordinated guanidinate group forms essentially a planar four-membered ring with the Yb atom within experimental errors. The bond angles around C(11) are consistent with sp² hybridization. The cent–Yb–cent (cent = the center of the cyclopentadienyl ring) plane relative to the YbNCN plane is approximately perpendicular. This disposition may result from the steric interaction between two bulky isopropyl groups and two cyclopentadienyl ligands. The C(11)–N(1) (1.297(10) Å) and C(11)–N(2) (1.303(9) Å) distances are approximately equivalent and significantly shorter

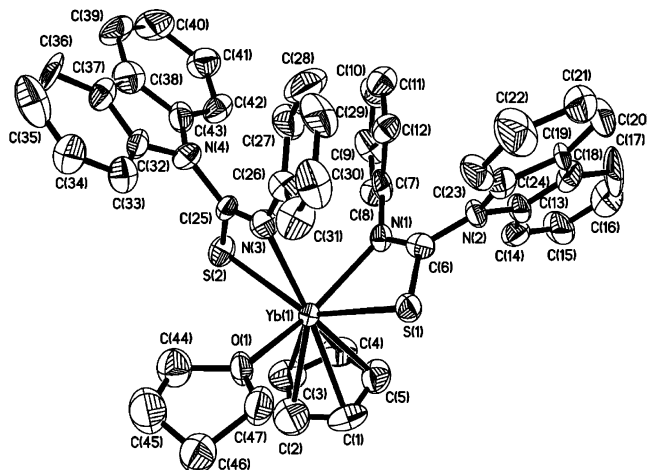


Figure 2. ORTEP diagram of **3** with the probability ellipsoids drawn at the 30% level. Hydrogen atoms are omitted for clarity.

Table 3. Bond Lengths (Å) and Angles (deg) for 3

Yb(1)–O(1)	2.365(13)	Yb(1)–S(1)	2.766(6)
Yb(1)–N(1)	2.390(7)	Yb(1)–C(6)	2.937(19)
Yb(1)–N(3)	2.532(8)	Yb(1)–C(25)	2.995(9)
Yb(1)–C(5)	2.580(15)	S(1)–C(6)	1.782(17)
Yb(1)–C(4)	2.597(14)	S(2)–C(25)	1.687(9)
Yb(1)–C(1)	2.600(18)	C(6)–N(1)	1.27(2)
Yb(1)–C(3)	2.628(16)	C(6)–N(2)	1.42(2)
Yb(1)–C(2)	2.630(17)	C(25)–N(3)	1.345(12)
Yb(1)–S(2)	2.709(5)	C(25)–N(4)	1.433(12)
O(1)–Yb(1)–N(1)	147.4(4)	C(6)–S(1)–Yb(1)	77.1(7)
O(1)–Yb(1)–N(3)	79.7(4)	C(25)–S(2)–Yb(1)	82.4(4)
N(1)–Yb(1)–N(3)	76.6(3)	N(1)–C(6)–N(2)	124.3(13)
N(1)–Yb(1)–S(2)	93.8(2)	N(1)–C(6)–S(1)	119.3(13)
N(3)–Yb(1)–S(2)	60.4(2)	N(2)–C(6)–S(1)	116.1(13)
N(1)–Yb(1)–S(1)	61.2(2)	N(1)–C(6)–Yb(1)	52.6(7)
N(3)–Yb(1)–S(1)	85.4(2)	N(2)–C(6)–Yb(1)	173.5(11)
N(1)–Yb(1)–C(6)	24.9(4)	S(1)–C(6)–Yb(1)	66.6(6)
N(3)–Yb(1)–C(6)	78.9(4)	C(6)–N(1)–Yb(1)	102.4(8)
S(2)–Yb(1)–C(6)	115.2(4)	N(3)–C(25)–S(2)	120.6(7)
S(1)–Yb(1)–C(6)	36.3(4)	N(4)–C(25)–S(2)	120.8(7)
N(1)–Yb(1)–C(25)	82.0(2)	N(3)–C(25)–Yb(1)	57.2(4)
N(3)–Yb(1)–C(25)	26.5(2)	N(4)–C(25)–Yb(1)	174.9(6)
S(2)–Yb(1)–C(25)	33.93(19)	S(2)–C(25)–Yb(1)	63.7(3)
S(1)–Yb(1)–C(25)	110.3(2)	C(25)–N(3)–Yb(1)	96.3(5)

than the C–N single-bond distances, indicating that the π-electrons of the C=N double bond in the present structure are delocalized over the N–C–N unit.¹⁵ Consistent with this case, the Yb–N(1) and Yb–N(2) distances, 2.292(6) and 2.305(6) Å, are intermediate between the values observed for the Yb–N single-bond distance and the Yb–N donor-bond distances (2.19–2.69 Å)¹⁶ and are comparable to the corresponding values found in [(C₅H₄Me)Yb(PzMe₂)(OSiMe₂PzMe₂)₂] (average 2.293(6) Å)^{16b} and {CyNC[N(SiMe₃)₂]NCy}₂YbN(SiMe₃)₂ (average 2.317(13) Å).¹⁷

Figure 2 shows the molecular structure of **3**. Selected bond distances and angles are listed in Table 3. The ytterbium atom carries one η⁵-cyclopentadienyl group

(15) Allen, F. H.; Kennard, O.; Watson, D. G.; Brammer, L.; Orpen, A. G. *J. Chem. Soc., Perkin Trans.* **1987**, S1.

(16) (a) Zhou, X. G.; Huang, Z. E.; Cai, R. F.; Zhang, L. X.; Hou, X. F.; Feng, X. J.; Huang, X. Y. *J. Organomet. Chem.* **1998**, 563, 101. (b) Zhou, X. G.; Ma, H. Z.; Huang, X. Y.; You, X. Z. *J. Chem. Soc., Chem. Commun.* **1995**, 2483. (c) Evans, W. J.; Drummond, D. K.; Chamberlain, L. A.; Doeden, R. J.; Bott, S. G.; Zhang, H.; Atwood, J. L. *J. Am. Chem. Soc.* **1988**, 110, 4983.

(17) Zhou, Y.; Yap, G. P. A.; Richeson, D. S. *Organometallics* **1998**, 17, 4387.

(14) Wilkins, J. D. *J. Organomet. Chem.* **1974**, 80, 349.

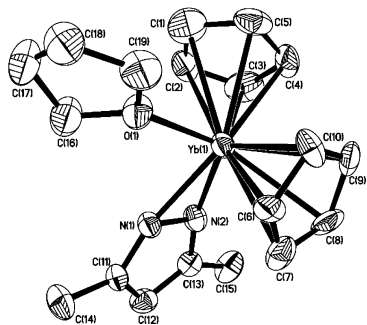


Figure 3. ORTEP diagram of **4** with the probability ellipsoids drawn at the 30% level. Hydrogen atoms are omitted for clarity.

Table 4. Selected Bond Lengths (Å) and Angles (deg) for 4

Yb(1)–N(2)	2.264(4)	Yb(1)–C(24)	2.575(3)
Yb(1)–N(1)	2.309(5)	Yb(1)–C(4)	2.582(3)
Yb(1)–O(1)	2.337(5)	Yb(1)–C(25)	2.588(3)
Yb(1)–C(28)	2.531(3)	Yb(1)–C(10)	2.607(3)
Yb(1)–C(29)	2.558(3)	Yb(1)–C(30)	2.610(3)
Yb(1)–C(27)	2.567(3)	Yb(1)–C(3)	2.616(3)
N(2)–Yb(1)–N(1)	35.11(15)	N(1)–Yb(1)–O(1)	82.70(18)
N(2)–Yb(1)–O(1)	116.39(15)		

and one THF molecule and is chelated by two SC(Cbz)NPh ligands. The most important feature of the structure is that two SC(Cbz)NPh ligands have distinctly different Yb–N and Yb–S distances. The Yb(1)–N(1) distance of 2.390(7) Å is significantly shorter than the Yb(1)–N(3) distance of 2.532(9) Å, while the Yb(1)–S(1) distance of 2.766(6) Å is longer than the Yb(1)–S(2) distance of 2.709(5) Å. This may be attributed to the large interligand steric interruption. Both N(1)–C(6)–S(1)–Yb(1) and N(3)–C(25)–S(2)–Yb(1) units are essentially planar within experimental error. All bond distances involving the ytterbium atom are in the normal ranges.^{16,18}

The overall structure of **4** is similar to that of the complex (C₅H₅)₂ErPzMe₂(THF)^{6e} (Figure 3). Selected bond distances and angles are given in Table 4. The ytterbium atom is coordinated to two η⁵-cyclopentadienyl groups, two nitrogen atoms of the 3,5-dimethylpyrazolate ligand, and one oxygen atom from the tetrahydrofuran molecule. The coordination number of the central metal Yb is 9. The Yb–N distances of 2.264(4) and 2.309(5) Å are in the range expected for an Ln–N bond interaction with partial single- and donor-bond character.¹⁶

As shown in Figure 4, complex **5** is a solvated monomer. Selected bond distances and angles are given in Table 5. It is interesting that the inserted PhNCO unit is bonded to the lanthanide ion only through oxygen, while the moiety in other PhNCO insertion products is generally η² bonded to the metal by oxygen and nitrogen.^{6d,13} This difference may be attributed to the stronger chelating coordination of the nitrogen atom of the pyrazolate group, which prohibits the bonding of the Yb³⁺ ion and the nitrogen atom of PhNCO. Consistent with this, in the mass spectrum of **5**, the loss of the PhNCO fragment occurs more readily than the direct loss of the PzMe₂ group. The cent–Yb–cent (cent

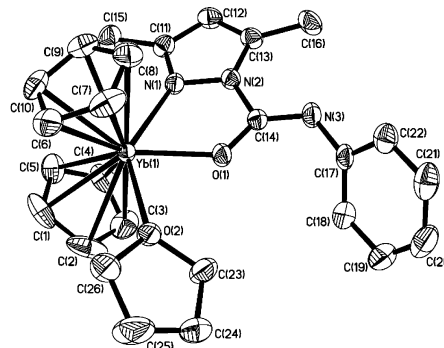


Figure 4. ORTEP diagram of **5** with the probability ellipsoids drawn at the 30% level. Hydrogen atoms are omitted for clarity.

Table 5. Selected Bond Lengths (Å) and Angles (deg) for 5

Yb(1)–O(1)	2.192(2)	Yb(1)–C(8)	2.627(4)
Yb(1)–O(2)	2.420(2)	Yb(1)–C(3)	2.632(4)
Yb(1)–N(1)	2.473(2)	Yb(1)–C(2)	2.632(4)
Yb(1)–C(5)	2.602(3)	O(1)–C(14)	1.269(3)
Yb(1)–C(7)	2.603(3)	N(1)–C(11)	1.328(4)
Yb(1)–C(1)	2.605(4)	N(1)–N(2)	1.376(3)
Yb(1)–C(6)	2.606(3)	N(2)–C(14)	1.434(4)
Yb(1)–C(4)	2.619(4)	N(3)–C(14)	1.269(4)
Yb(1)–C(10)	2.623(3)	N(3)–C(17)	1.403(4)
O(1)–Yb(1)–O(2)	73.91(7)	N(1)–N(2)–C(14)	117.1(2)
O(1)–Yb(1)–N(1)	66.31(8)	C(14)–N(3)–C(17)	120.0(3)
C(14)–O(1)–Yb(1)	129.3(2)	N(3)–C(14)–O(1)	130.7(3)
N(2)–N(1)–Yb(1)	112.22(17)	N(3)–C(14)–N(2)	116.1(3)
C(13)–N(2)–N(1)	110.9(3)	O(1)–C(14)–N(2)	113.2(3)
C(13)–N(2)–C(14)	131.9(3)		

= the center of cyclopentadienyl ring) plane relative to the Yb–N(1)–O(1) plane is approximately perpendicular (89.3°). The cent–Yb–cent angle is 137.2°. The N(3)–C(14) distance (1.269(4) Å) is comparable to the accepted value for the N(sp²)=C(sp²) double bond (1.28 Å).¹⁹ The Yb–N(1) distance (2.473(2) Å) is comparable to the values observed for the Yb–N donor-bond distance¹⁶ and is slightly and significantly longer than the corresponding values found in [(C₅H₄Me)Yb(PzMe₂)(OSiMe₂PzMe₂)₂] (Yb–N(bridge pyrazolate) = 2.402(7) Å).^{16b} The Yb–O(1) distance (2.192(2) Å) is smaller than the corresponding values found in [(C₅H₄Me)Yb(PzMe₂)(OSiMe₂PzMe₂)₂] (Yb–O = 2.250(5) Å).^{16b} The Yb–O(THF) distance (2.420(2) Å) is longer than the corresponding value in **3** (2.365(13) Å).^{16c}

All the Yb–C(Cp) distances in these complexes are in the normal ranges observed for lanthanocene complexes.²⁰

Conclusions

The present results demonstrate that *N,N*-diisopropylcarbodiimide can insert into the Yb–N bond of (C₅H₅)₂YbCbz(THF) (**1**) under mild conditions but it does not react with (C₅H₅)₂YbPzMe₂(THF) even under more rigorous conditions, which is different from the results reported for organolanthanide amido complexes. PhNCS is also found to insert into the Yb–N(Cbz) bond of **1**. Interestingly, the insertion product derived from PhNCS

(19) March, J. In *Advanced Organic Chemistry*; McGraw-Hill: New York, 1997; Vol. 2, p 24.

(20) (a) Zhou, X. G.; Wu, Z. Z.; Jin, Z. S. *J. Organomet. Chem.* **1992**, *431*, 289. (b) Evans, W. J.; Dominguez, R.; Hanusa, T. P. *Organometallics* **1986**, *5*, 263.

(18) Zalkin, A.; Henly, T. J.; Anderson, R. A. *Acta Crystallogr.* **1987**, *C43*, 233.

with **1** is unstable at room temperature and rearranges easily to the unexpected $(C_5H_5)Yb[S\cdots C(Cbz)\cdots NPh]_2$ (THF), revealing an unusual rearrangement reaction of cyclopentadienyl lanthanide complexes. Furthermore, the insertion of phenyl isocyanate into the Yb–N(η^2 -pyrazolate) bond presents the first example of unsaturated organic molecule insertion into the Ln–N(η^2) bond of the chelating pyrazolate complexes. However, in contrast to the reactivity of organolanthanide amido complexes, where the monoinsertion product catalyzed excess PhNCO to form a polymer, in the present case, no further reaction was observed. All observed differences indicate that organolanthanides containing aromatic nitrogen ligands exhibit lower activity to *N,N*-diisopropylcarbodiimide, phenyl isothiocyanate, and phenyl isocyanate compared with the corresponding

amido complexes. These reactions provide a new strategy for introducing a substituent at the nitrogen atom of organic heterocyclic compounds.

Acknowledgment. We thank the National Natural Science Foundation of China and the Research Funds of Excellent Young Teacher and the New Century Distinguished Scientist of National Education Ministry of China for financial support.

Supporting Information Available: Tables of atomic coordinates and thermal parameters and all bond distances and angles for complexes **2–5**; these data are also available as CIF files. This material is available free of charge via the Internet at <http://pubs.acs.org>.

OM0340342